

Spin pumping into quantum spin nematic states

Takuto Ishikawa,¹ Wolfgang Belzig,² and Takeo Kato¹

¹*Institute for Solid State Physics, University of Tokyo, Kashiwa 277-8581, Japan*

²*Physics Department, University of Konstanz, 78457 Konstanz, Germany*

We theoretically study spin pumping into a spin-nematic state in a junction system composed of a ferromagnetic insulator and a spin-nematic insulator, described by using the spin-1 bilinear-biquadratic model. We analyze an increase of the Gilbert damping in ferromagnetic resonance (FMR) due to an interfacial exchange coupling within a mean-field theory based on the Schwinger boson method. We find that the two Schwinger bosons contribute in distinct ways to spin pumping. We report a detailed dependence of the spin pumping on a resonant frequency, a magnetic field, and an interface type.

I. INTRODUCTION

In the development of spintronics, the technique of spin pumping driven by ferromagnetic resonance (FMR) has emerged as a versatile tool for injecting spins into materials adjacent to ferromagnets [1–6]. Spin pumping can also serve as a probe for spin excitations of target materials through the Gilbert damping, which can be extracted from the width of the FMR peak. In fact, enhancement of the Gilbert damping due to interfacial coupling with target materials has been shown to contain valuable information regarding their spin excitations [7–27].

Spin pumping into exotic materials with hidden orders represents a significant challenge in identifying novel states of matter and understanding their quantum nature. Among these exotic hidden orders, the spin-nematic state, characterized by spin-rotation symmetry breaking without any accompanying magnetic order, stands as a representative example. The spin-nematic state is described by quadrupolar order or higher multipolar order and has been extensively studied theoretically, using models such as the bilinear-biquadratic exchange model [28–37] and the J_1 - J_2 frustrated model [38–51], and the dimer model [52–55]. These theoretical models predict the existence of ferro- or antiferro-quadrupolar states. The realization of the spin nematic state has also been discussed in a variety of materials such as LiCuVO_4 [56–58] and $\text{BaCdVO}(\text{PO}_4)_2$ [59–61]. Recently, a study of the spin Seebeck effect in the spin-nematic state has also been conducted [62].

In this work, we theoretically calculate the enhancement of Gilbert damping resulting from spin pumping into a spin-nematic insulator. We consider a magnetic junction composed of a spin-nematic (SN) insulator and a ferromagnetic insulator (FI) subjected to microwave irradiation (see Fig. 1). To discuss qualitative features of spin pumping, we employ a simple model based on the bilinear-biquadratic exchange model to realize the spin-nematic state. We derive an analytical expression for the enhancement of the Gilbert damping by second-order perturbation theory with respect to interface coupling and the Schwinger-boson mean-field method. Furthermore, we examine how the enhancement of Gilbert damping depends on the FMR frequency, magnetic field,

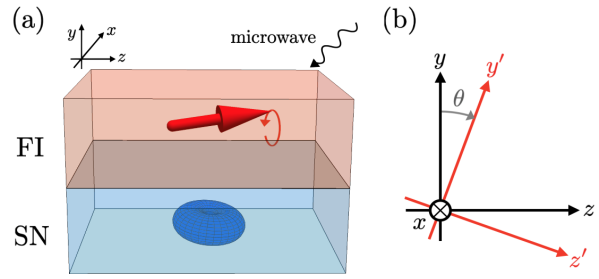


FIG. 1. (a) Magnetic junction composed of a ferromagnetic insulator (FI) and a spin nematic (SN) insulator. (b) Coordinate transformation between the laboratory coordinates (x, y, z) and the magnetization-fixed coordinates (x', y', z') .

and interface type.

The rest of this work is organized as follows. In Sec. II, we introduce our theoretical model for a FI/SN junction system and explain the Schwinger-boson mean-field theory for the spin-nematic phase. In Sec. III, we theoretically calculate the enhancement of Gilbert damping due to interfacial exchange coupling within second-order perturbation. In Sec. IV, we show how the increase of Gilbert damping depends on the orientation and strength of the external magnetic field for both clean and dirty interfaces. Finally, we summarize our results in Sec. V. Appendix A is devoted to a detailed derivation of analytic expressions.

II. MODEL

We consider a junction system composed of a ferromagnetic insulator (FI) and a spin-nematic insulator (SN). The model Hamiltonian is expressed as

$$\mathcal{H} = \mathcal{H}_{\text{FI}} + \mathcal{H}_{\text{SN}} + \mathcal{H}_{\text{int}}, \quad (1)$$

where \mathcal{H}_{FI} , \mathcal{H}_{SN} , and \mathcal{H}_{int} represent FI, SN, and an interfacial exchange coupling. Explicit forms of each Hamiltonian are provided in the following subsections.

A. Ferromagnetic insulator (FI)

To describe the FI, we consider the Heisenberg model with axial anisotropy, whose Hamiltonian is expressed as.

$$\mathcal{H}_{\text{FI}} = J \sum_{\langle i,j \rangle} \mathcal{S}_i \cdot \mathcal{S}_j - \lambda_L \sum_i (\mathcal{S}_i^z)^2, \quad (2)$$

where \mathcal{S}_i is a localized spin with amplitude of S_0 , $J (< 0)$ is a ferromagnetic exchange coupling, $\langle i,j \rangle$ indicates a pair of neighboring sites, and λ_L denotes the strength of the axial anisotropy. For simplicity, we assume that the anisotropy energy proportional to λ_L is much larger than the Zeeman energy induced by an external magnetic field. Consequently, the spin polarization in the FI is aligned along the z -axis throughout this paper. Using the Holstein-Primakoff transformation and the independent magnon approximation, the Hamiltonian of the FI is rewritten in the long-wavelength approximation as $\mathcal{H}_{\text{FI}} = \sum_{\mathbf{k}} \hbar \omega_{\mathbf{k}} b_{\mathbf{k}}^\dagger b_{\mathbf{k}}$, where $b_{\mathbf{k}}$ ($b_{\mathbf{k}}^\dagger$) is the annihilation (creation) operator of magnons with wavenumber \mathbf{k} , $\omega_{\mathbf{k}} = 2S_0\lambda_L + \mathcal{D}k^2$ is a magnon dispersion, and \mathcal{D} is a spin stiffness. Since the external microwave induces a uniform spin precession, it is sufficient to consider the Hamiltonian for $\mathbf{k} = \mathbf{0}$:

$$\mathcal{H}_{\text{FI}} = \hbar \omega_0 b_0^\dagger b_0, \quad (3)$$

where $\omega_0 = 2S_0\lambda_L$.

B. Spin-nematic (SN) state

As a simple model to realize the spin-nematic state, we consider a spin-1 bilinear-biquadratic model on a triangular lattice, whose Hamiltonian is given as

$$\mathcal{H}_{\text{SN}} = \sum_{\langle i,j \rangle} [J_1 \mathcal{S}_i \cdot \mathcal{S}_j + J_2 (\mathcal{S}_i \cdot \mathcal{S}_j)^2] - h \sum_i \mathcal{S}_i^{z'}, \quad (4)$$

where \mathcal{S}_i denotes a localized spin, J_1 and J_2 denote the strengths of the bilinear and biquadratic couplings, respectively, and h represents an external magnetic field. For simplicity in the calculation, we introduced a new coordinate (x', y', z') , to the original ordinate as

$$\begin{pmatrix} x \\ y \\ z \end{pmatrix} = \begin{pmatrix} 1 & 0 & 0 \\ 0 & \cos \theta & -\sin \theta \\ 0 & \sin \theta & \cos \theta \end{pmatrix} \begin{pmatrix} x' \\ y' \\ z' \end{pmatrix}, \quad (5)$$

and the external magnetic field is applied along the z' direction (see Fig. 1(b)). This bilinear-biquadratic model is known to exhibit ferromagnetic quadrupole ordering (spin-nematic phase) within a finite range of the ratio J_1/J_2 [63]. To construct a mean-field theory for the spin-nematic phase, we introduce the operators of the SU(3)

Schwinger boson as follows [34, 36]:

$$S_i^{x'} = -i[a_{y'}^\dagger(i)a_{z'}(i) - a_{z'}^\dagger(i)a_{y'}(i)], \quad (6)$$

$$S_i^{y'} = -i[a_{z'}^\dagger(i)a_{x'}(i) - a_{x'}^\dagger(i)a_{z'}(i)], \quad (7)$$

$$S_i^{z'} = -i[a_{x'}^\dagger(i)a_{y'}(i) - a_{y'}^\dagger(i)a_{x'}(i)]. \quad (8)$$

In the absence of an external magnetic field, a mean-field theory for the spin nematic state is constructed by replacing one of the Schwinger bosons with its mean value. The direction of the ferro-quadrupolar state, i.e., the component of the condensed Schwinger bosons, is perpendicular to the magnetic field. In our calculation, we assume that condensation occurs for the y' -component boson denoted as

$$a_{y'}(i), a_{y'}^\dagger(i) \rightarrow \sqrt{M - a_{x'}^\dagger(i)a_{x'}(i) - a_{z'}^\dagger(i)a_{z'}(i)}, \quad (9)$$

where M represents the saturation amplitude of the quadrupole ordering. Although M equals the magnitude of the localized spin, i.e. $M = 1$ for the spin-1 system, we treat M as a control parameter.

In the presence of an external magnetic field in the z' direction, the quadrupole ordering loses the axial symmetry around the y' axis. Therefore, we need to prepare new Schwinger bosons as

$$\begin{pmatrix} a_{x'}^\dagger \\ a_{y'}^\dagger \\ a_{z'}^\dagger \end{pmatrix} = \begin{pmatrix} \cos \frac{\mu}{2} & i \sin \frac{\mu}{2} & 0 \\ i \sin \frac{\mu}{2} & \cos \frac{\mu}{2} & 0 \\ 0 & 0 & 1 \end{pmatrix} \begin{pmatrix} a_{\perp}^\dagger \\ a_{\parallel}^\dagger \\ a_{z'}^\dagger \end{pmatrix}, \quad (10)$$

with a finite magnetic moment $m = M \sin \mu$, and then assume condensation of the boson operator a_{\parallel} as

$$a_{\parallel}(i), a_{\parallel}^\dagger(i) \rightarrow \sqrt{M - a_{\perp}^\dagger(i)a_{\perp}(i) - a_{z'}^\dagger(i)a_{z'}(i)}. \quad (11)$$

The magnetization is proportional to the magnetic field from the mean field result,

$$m = \frac{h}{z(J_1 - J_2)} \quad (12)$$

where z ($= 6$) is the number of nearest neighbor sites. By expanding the Hamiltonian with respect to $a_{z'}$, a_{\perp} , and their Hermite conjugates and by leaving the leading contribution with respect to $1/M$, the Hamiltonian is approximately rewritten as

$$\mathcal{H}_{\text{SN}} = \frac{zM}{2} \sum_{\nu=\perp,z'} \sum_{\mathbf{k}} \left\{ 2A_{\mathbf{k}\nu} a_{\mathbf{k}\nu}^\dagger a_{\mathbf{k}\nu} + B_{\mathbf{k}\nu} [a_{\mathbf{k}\nu} a_{-\mathbf{k}\nu} + a_{\mathbf{k}\nu}^\dagger a_{-\mathbf{k}\nu}^\dagger] \right\}, \quad (13)$$

where the coefficients are given as

$$A_{\mathbf{k}z'} = J_1 \gamma_{\mathbf{k}} - J_2, \quad (14)$$

$$B_{\mathbf{k}z'} = (J_2 - J_1) \cos \mu \gamma_{\mathbf{k}}, \quad (15)$$

$$A_{\mathbf{k}\perp} = (J_1 \cos^2 \mu + J_2 \sin^2 \mu) \gamma_{\mathbf{k}} - J_2, \quad (16)$$

$$B_{\mathbf{k}\perp} = (J_2 - J_1) \cos^2 \mu \gamma_{\mathbf{k}}, \quad (17)$$

$$\gamma_{\mathbf{k}} = \frac{1}{z} \sum_{\delta} e^{i\mathbf{k} \cdot \mathbf{r}_{\delta}}, \quad (18)$$

where \mathbf{r}_δ denotes a displacement vector spanning a site to its neighboring site δ . This Hamiltonian can be diagonalized by the Bogoliubov transformation,

$$a_{\mathbf{k}\nu}^\dagger = \cosh \xi_{\mathbf{k}\nu} \alpha_{\mathbf{k}\nu}^\dagger + \sinh \xi_{\mathbf{k}\nu} \alpha_{-\mathbf{k}\nu}, \quad (19)$$

$$a_{\mathbf{k}\nu} = \cosh \xi_{\mathbf{k}\nu} \alpha_{\mathbf{k}\nu} + \sinh \xi_{\mathbf{k}\nu} \alpha_{-\mathbf{k}\nu}^\dagger, \quad (20)$$

where $\xi_{\mathbf{k}\nu}$ is chosen to satisfy

$$\tanh(2\xi_{\mathbf{k}\nu}) = -\frac{B_{\mathbf{k}\nu}}{A_{\mathbf{k}\nu}}. \quad (21)$$

By dropping a constant term, we finally obtain the following Hamiltonian:

$$\mathcal{H}_{\text{SN}} = \sum_{\nu=z',\perp} \sum_{\mathbf{k}} \varepsilon_{\mathbf{k}\nu} \alpha_{\mathbf{k}\nu}^\dagger \alpha_{\mathbf{k}\nu}, \quad (22)$$

where $\varepsilon_{\mathbf{k}\nu}$ is a dispersion of the Schwinger bosons given as

$$\varepsilon_{\mathbf{k}}^\nu = \frac{zM}{2} \sqrt{A_{\mathbf{k}\nu}^2 - B_{\mathbf{k}\nu}^2}, \quad (\nu = z', \perp). \quad (23)$$

C. Interfacial exchange coupling

We consider the exchange coupling at the FI/SN interface, with Hamiltonian is given as

$$\mathcal{H}_{\text{int}} = \sum_{\mathbf{k}, \mathbf{k}'} (T_{\mathbf{k}, \mathbf{k}'} \mathcal{S}_{\mathbf{k}}^- \mathcal{S}_{\mathbf{k}'}^+ + T_{\mathbf{k}, \mathbf{k}'}^* \mathcal{S}_{\mathbf{k}}^+ \mathcal{S}_{\mathbf{k}'}^-), \quad (24)$$

where $\mathcal{S}_{\mathbf{k}}^\pm = \mathcal{S}_{\mathbf{k}}^x \pm i\mathcal{S}_{\mathbf{k}}^y$ and $\mathcal{S}_{\mathbf{k}}^\pm = \mathcal{S}_{\mathbf{k}}^{x'} \pm i\mathcal{S}_{\mathbf{k}}^{y'}$ are Fourier transformations of the spin ladder operators in the FI and the SN, respectively. Since we focus on the uniform spin precession in the FI, the coupling at the interface is approximated as

$$\mathcal{H}_{\text{int}} = \sqrt{2S_0} \sum_{\mathbf{k}'} (T_{\mathbf{0}, \mathbf{k}'} b_0^\dagger \mathcal{S}_{\mathbf{k}'}^+ + T_{\mathbf{0}, \mathbf{k}'}^* b_0 \mathcal{S}_{\mathbf{k}'}^-). \quad (25)$$

We should note that the spin ladder operators are defined in the laboratory coordinates (x, y, z) , which are related to the coordinates (x', y', z') as

$$\begin{pmatrix} S_i^x \\ S_i^y \\ S_i^z \end{pmatrix} = \begin{pmatrix} 1 & 0 & 0 \\ 0 & \cos\theta & -\sin\theta \\ 0 & \sin\theta & \cos\theta \end{pmatrix} \begin{pmatrix} S_i^{x'} \\ S_i^{y'} \\ S_i^{z'} \end{pmatrix}. \quad (26)$$

In our study, we consider two types of the FI/SN interface, i.e., a dirty and clean interface:

$$\text{dirty interface} : T_{\mathbf{0}, \mathbf{k}'} = \bar{T}, \quad (27)$$

$$\text{clean interface} : T_{\mathbf{0}, \mathbf{k}'} = \bar{T} \delta_{\mathbf{k}', \mathbf{0}}. \quad (28)$$

We note that only the uniform spin component in the spin-nematic insulator is excited by spin pumping for the clean interface due to the momentum conservation law.

III. FORMULATION

In this section, we formulate the Gilbert damping in the FMR experiment for the FI/SN bilayer system. First, we briefly describe a general formulation in Sec. III A. Next, we calculate the increase of the Gilbert damping for the dirty and clean interfaces in Sec. III B and Sec. III C, respectively.

A. Gilbert damping

We first define the temperature Green's function for magnons in the FI as follows:

$$\begin{aligned} G(\tau) &= -\frac{1}{\hbar} \langle S_0^+(\tau) S_0^-(0) \rangle \\ &= -\frac{2S_0}{\hbar} \langle b_0(\tau) b_0^\dagger(0) \rangle, \end{aligned} \quad (29)$$

$$G(i\omega_n) = \int_0^{\hbar\beta} d\tau e^{i\omega_n\tau} G(\tau), \quad (30)$$

where $A(\tau) = e^{\mathcal{H}\tau} A e^{-\mathcal{H}\tau}$, $\omega_n = 2\pi n k_B T / \hbar$ is the bosonic Matsubara frequency, and β is the inverse temperature. Using linear response theory, we can show that the microwave absorption rate is proportional to $\text{Im } G^R(\omega)$, where $G^R(\omega) = G(i\omega_n \rightarrow \omega + i\delta)$ is a retarded component of the spin correlation function [21]. For an isolated FI, the retarded Green's function is calculated as

$$G_0^R(\omega) = \frac{2S_0/\hbar}{\omega - \omega_0 + i\alpha_G}, \quad (31)$$

where we introduce a phenomenological damping constant, α_G , to describe the Gilbert damping in the bulk FI.

In the presence of exchange coupling between the FI and the spin-nematic insulator, the retarded Green's function is modified as

$$G^R(\omega) = \frac{2S_0/\hbar}{\omega - \omega_0 + i\alpha_G - \Sigma^R(\omega)}, \quad (32)$$

where $\Sigma^R(\omega)$ is the retarded component of the self-energy due to the interface, which is obtained by the analytic continuation $\Sigma^R(\omega) = \Sigma(i\omega_n \rightarrow \omega + i\delta)$ from the self-energy in the imaginary-time formalism, $\Sigma(i\omega_n)$. Assuming the FMR peak is sufficiently sharp, the increase of the Gilbert damping is well approximated as

$$\delta\alpha_G = -\frac{2S_0}{\hbar\omega_0} \text{Im } \Sigma^R(\omega_0). \quad (33)$$

We note that the real part of the self-energy corresponds to the shift of the FMR frequency [25]. Although this change in FMR frequency is expected to include information on the spin-nematic phase, we only focus on the modulation of the Gilbert damping for simplicity in the discussion.

Within the second-order perturbation with respect to \mathcal{H}_{int} , the self-energy in the imaginary-time formalism is calculated as

$$\Sigma(i\omega_n) = \int_0^{\hbar\beta} d\tau e^{i\omega_n\tau} \Sigma(\tau), \quad (34)$$

$$\Sigma(\tau) = - \sum_{\mathbf{k}, \mathbf{k}'} \frac{T_{\mathbf{0}, \mathbf{k}} T_{\mathbf{0}, \mathbf{k}'}^*}{\hbar} \langle S_{\mathbf{k}}^+(\tau) S_{\mathbf{k}'}^-(0) \rangle, \quad (35)$$

where the average is taken for thermal equilibrium of the spin-nematic state. Using the coordinate transformation given in Eq. (26), the self-energy is obtained as

$$\begin{aligned} \Sigma(\tau) = & - \sum_{a, b=1}^3 \sum_{\mathbf{k}, \mathbf{k}'} \frac{T_{\mathbf{0}, \mathbf{k}} T_{\mathbf{0}, \mathbf{k}'}^*}{\hbar} g_a(\theta) g_b^*(\theta) \\ & \times \left\langle S_{\mathbf{k}}^{(a)}(\tau) \left\{ S_{\mathbf{k}'}^{(b)}(0) \right\}^\dagger \right\rangle, \end{aligned} \quad (36)$$

where

$$S_{\mathbf{k}}^{(1)} = S_{\mathbf{k}}^{z'}, \quad g_1(\theta) = -i \sin \theta, \quad (37)$$

$$S_{\mathbf{k}}^{(2)} = S_{\mathbf{k}}^{+'}, \quad g_2(\theta) = \cos^2(\theta/2), \quad (38)$$

$$S_{\mathbf{k}}^{(3)} = S_{\mathbf{k}}^{-'}, \quad g_3(\theta) = \sin^2(\theta/2). \quad (39)$$

B. Dirty interface

For the model of the dirty interface given in Eq. (27), the self-energy is written as

$$\Sigma(\tau) = - \sum_{a, b=1}^3 \sum_{\mathbf{k}, \mathbf{k}'} \frac{|\bar{T}|^2}{\hbar} g_a(\theta) g_b(\theta) \left\langle S_{\mathbf{k}}^{(a)}(\tau) \left\{ S_{\mathbf{k}'}^{(b)}(0) \right\}^\dagger \right\rangle. \quad (40)$$

Using the imaginary-time spin-spin correlation function

$$\chi_{\mathbf{k}, \mathbf{k}'}^{\mu\nu}(\tau) = -\frac{1}{\hbar} \langle S_{\mathbf{k}}^\mu(\tau) S_{\mathbf{k}'}^\nu(0) \rangle, \quad (\mu, \nu = z', +', -'), \quad (41)$$

the self-energy is rewritten as

$$\begin{aligned} \Sigma(\tau) = & \sum_{\mathbf{k}} \frac{|\bar{T}|^2}{\hbar} \left\{ \sin^2 \theta \chi_{\mathbf{k}, -\mathbf{k}}^{z' z'}(\tau) \right. \\ & + \cos^4(\theta/2) \chi_{\mathbf{k}, -\mathbf{k}}^{+' -'}(\tau) + \sin^4(\theta/2) \chi_{\mathbf{k}, -\mathbf{k}}^{-' +'(\tau)} \\ & \left. + \frac{1}{4} \sin^2 \theta [\chi_{\mathbf{k}, -\mathbf{k}}^{+' +'}(\tau) + \chi_{\mathbf{k}, -\mathbf{k}}^{-' -'}(\tau)] \right\}, \end{aligned} \quad (42)$$

where we have used translational invariance of \mathcal{H}_{SN} and $\chi^{z' +'} = \chi^{z' -'} = \chi^{+' z'} = \chi^{-' z'} = 0$. Here, it is remarkable that $\chi_{\mathbf{k}, -\mathbf{k}}^{-' -'}(\tau)$ and $\chi_{\mathbf{k}, -\mathbf{k}}^{+' +'}(\tau)$ does not vanish.

The remaining task is to calculate the spin-spin correlation function $\chi_{\mathbf{k}, -\mathbf{k}}^{\mu\nu}(\tau)$ and its Fourier transformation. This is done by simple calculation using the mean-field Hamiltonian, Eq. (22), written in terms of the Schwinger

bosons. A detailed calculation is given in Appendix A. Consequently, the increase of the Gilbert damping for $\omega_0 > 0$ is given as

$$\delta\alpha_G = \frac{2\pi S_0 |\bar{T}|^2}{\hbar\omega_0} \sum_{\mathbf{k}} \sum_{\nu=z, \perp} C_\nu \delta(\hbar\omega_0 - \varepsilon_{\mathbf{k}\nu}), \quad (43)$$

where

$$\begin{aligned} C_z = & M \left[\sin \mu \cos \theta \right. \\ & + \{\cosh 2\xi_z(\mathbf{k}) - \cos \mu \sinh 2\xi_z(\mathbf{k})\} \cos^2 \theta \\ & \left. + \frac{1 + \cos \mu}{2} \{\cosh 2\xi_z(\mathbf{k}) - \sinh 2\xi_z(\mathbf{k})\} \sin^2 \theta \right], \end{aligned} \quad (44)$$

$$C_\perp = M \cos^2 \mu [\cosh(2\xi_{\mathbf{k}\perp}) - \sinh(2\xi_{\mathbf{k}\perp})] \sin^2 \theta. \quad (45)$$

C. Clean interface

The result for a clean interface is easily obtained by restricting the sum of the wavenumber to $\mathbf{k} = \mathbf{0}$. Noting that $\varepsilon_{\mathbf{0}\perp} = 0$, the increase of the Gilbert damping for $\omega_0 > 0$ is given as

$$\delta\alpha_G = \frac{2\pi S_0 |\bar{T}|^2}{\hbar\omega_0} C'_z \delta(\hbar\omega_0 - \varepsilon_{\mathbf{0}z}), \quad (46)$$

$$\begin{aligned} C'_z = & M \left[\sin \mu \cos \theta \right. \\ & + \{\cosh 2\xi_0 - \cos \mu \sinh 2\xi_0\} \cos^2 \theta \\ & \left. + \frac{1 + \cos \mu}{2} \{\cosh 2\xi_0 - \sinh 2\xi_0\} \sin^2 \theta \right], \end{aligned} \quad (47)$$

where $\xi_0 = \xi_{\mathbf{k}=\mathbf{0}z}$.

IV. RESULT

In this section, we present the results for the increase of the Gilbert damping in the FI/SN bilayer system. First, we show the results in the absence of a magnetic field ($\mu = 0$) in Sec. IV A. Next, we discuss the effect of a finite magnetic field ($\mu > 0$) for the dirty and clean interfaces in Sec. IV B and Sec. IV C, respectively. Throughout this paper, the parameters are set as $J_1 = 0$ and $J_2 = -\mathcal{J}$, which stabilizes the spin-nematic state. Furthermore, we replace the delta-function in Eqs. (43) and (46) with the Lorentzian function of width $0.03\mathcal{J}$ to plot the dependence on the FMR frequency ω_0 . We note that $\delta\alpha_G$ becomes temperature-independent within the mean-field theory, which is justified at low temperatures.

A. Zero magnetic field

The increase of the Gilbert damping significantly depends on whether the interface is clean or dirty. In the case of a clean interface, the Gilbert damping is

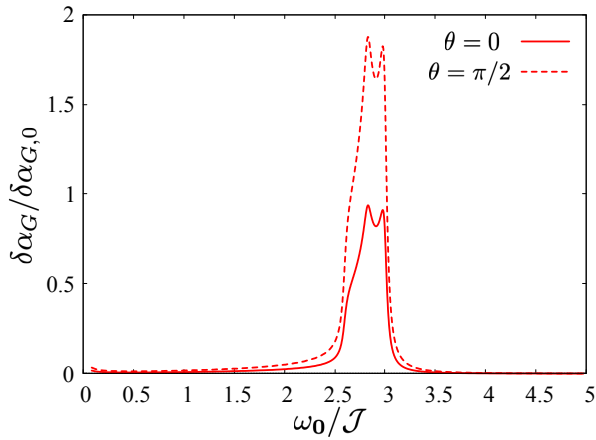


FIG. 2. The increase of the Gilbert damping for the dirty interface as a function of the FMR frequency ω_0 . The parameters are set as $J_1 = 0$, $J_2 = -\mathcal{J}$, and $h = 0$. The solid and dashed lines represent $\theta = 0$ and $\theta = \pi/2$, respectively.

not modulated, that is, $\delta\alpha_G = 0$ because the coefficient in Eq. (46) becomes zero. In contrast, for a dirty interface, $\delta\alpha_G$ has a finite value. In Fig. 2, we plot $\delta\alpha_G/\delta\alpha_{G,0}$ as a function of the FMR frequency ω_0 , where $\delta\alpha_{G,0} = 2\pi S_0 |\bar{T}|^2 \mathcal{A}/\mathcal{J}^2$ is a normalization factor. As shown in the figure, the enhancement of Gilbert damping for $\theta = \pi/2$ is twice that of $\theta = 0$. In general, $\delta\alpha_G$ is proportional to $1 + \sin^2 \theta$. This dependence arises from the fact that $\delta\alpha_G$ is a sum of the two contributions from two types of Schwinger bosons; the contribution of the z' -component Schwinger bosons is independent of θ , while that of the x' -component Schwinger bosons is proportional to $\sin^2 \theta$ (see also Eqs. (43)-(45)).

B. Dirty interface under a finite magnetic field

Fig. 3(a) shows $\delta\alpha_G/\delta\alpha_{G,0}$ as a function of the FMR frequency ω_0 in the presence of an external magnetic field. As the magnetic field increases, $\delta\alpha_G(\omega_0)$ grows because the net magnetization in the spin-nematic insulator increases and the peak becomes sharper reflecting changes in the dispersion relation of the Schwinger bosons (see also Fig. 4(d)-(f)). Fig. 3(b) shows the increase of the Gilbert damping at $\theta = 0$, $\theta = \pi/2$, $\theta = \pi$ with the magnetic field fixed at $h = 3\mathcal{J}$, where the contributions of the two kinds of Schwinger bosons are plotted separately. We note that the contribution from the perpendicular Schwinger bosons vanishes for $\theta = 0, \pi$. The peak at $\omega_0 = 2.9\mathcal{J}$ is the contribution of the z' -component Schwinger bosons, and the peak at $\omega_0 = 3.2\mathcal{J}$ is that of the perpendicular component of the Schwinger bosons. As seen in the figure, the two components of the bosons have different dependencies on θ .

To clarify the dependence on the magnetic-field orientation, we show the increase of the Gilbert damping as a

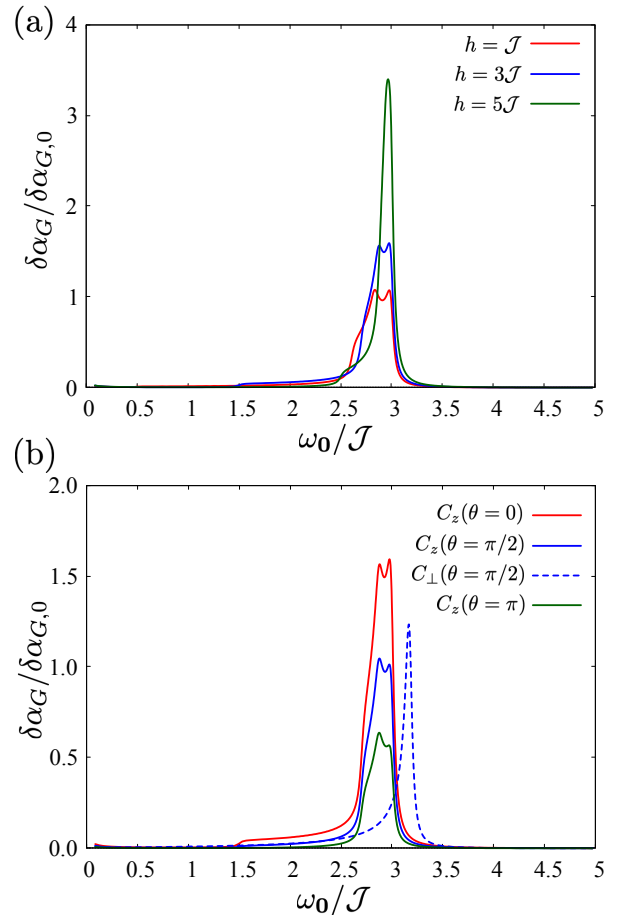


FIG. 3. The increase of the Gilbert damping for the dirty interface is shown as a function of the FMR frequency ω_0 for $J_1 = 0$ and $J_2 = -\mathcal{J}$. (a) The magnetic-field dependence at $\theta = 0$. The three curves correspond to $h = \mathcal{J}$, $3\mathcal{J}$, and $5\mathcal{J}$, respectively. (b) The angle dependence at $h = 3\mathcal{J}$. The red, blue, and green solid lines correspond to the contribution of C_z for $\theta = 0$, $\theta = \pi/2$, and $\theta = \pi$, respectively. The dashed line represents the contribution of C_\perp at $\theta = \pi/2$. We note that $C_\perp(\theta = 0) = C_\perp(\theta = \pi) = 0$.

function of ω_0 and θ for $h = \mathcal{J}$, $3\mathcal{J}$, and $5\mathcal{J}$ in Fig. 4 (a), (b), and (c), respectively. The peak height at a finite frequency varies as the angle θ changes. The shape and position of the peak of $\delta\alpha_G$ are determined by the corresponding dispersion of the two Schwinger bosons, $\varepsilon_{\mathbf{k}\nu}$, as shown in Fig. 4(d)-(f). As expected from the form of Eq. (43), the peak frequency of $\delta\alpha_G$ corresponds to the energy of the flat part in the dispersion of the Schwinger bosons. The low-frequency shoulder structure of $\delta\alpha_G$ reflects the low-energy states of the Schwinger bosons, though its weight is much weaker than that of the main peak.

Let us examine the detailed features for each strength of the magnetic field. For $h = \mathcal{J}$, the dispersions of the two Schwinger bosons are almost identical except for the

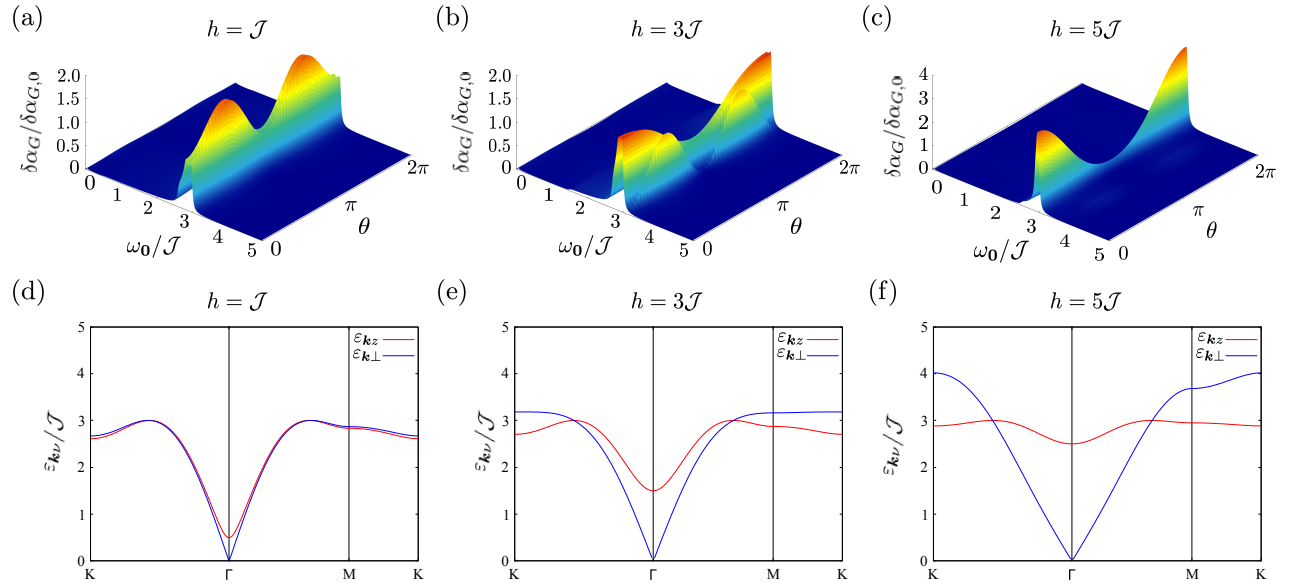


FIG. 4. The top row shows the increase of the Gilbert damping for the dirty interface as a function of the FMR frequency ω_0 and θ . The bottom row shows the dispersion of the Schwinger bosons of $\varepsilon_{\mathbf{k}z}$ and $\varepsilon_{\mathbf{k}\perp}$. The parameters are set as $J_1 = 0$ and $J_2 = -\mathcal{J}$. In each row, figures are arranged from left to right, $h = \mathcal{J}$, $h = 3\mathcal{J}$, and $h = 5\mathcal{J}$.

Γ point, as shown in Fig. 4(d). As a result, $\delta\alpha_G$ has a single peak and becomes significant near $\theta = \pi/2, 3\pi/2$ as shown in Fig. 4(a). For a higher magnetic field of $h = 3\mathcal{J}$, a new high-energy peak appears as shown in Fig. 4(b). The low-energy peak around $\omega_0 = 2.9\mathcal{J}$ becomes significant near $\theta = 0$, while the high-energy peak around $\omega_0 = 3.2\mathcal{J}$ appears around $\theta = \pi/2, 3\pi/2$. This behavior reflects the dispersion relations of the two Schwinger bosons as shown in Fig. 4(e). The positions of the double peaks correspond to the flat bands, whose energies are different for the two types of bosons, while their weights have a different dependencies on θ , as seen also in Eqs. (43)-(45). Fig. 4(c) shows the increase of the Gilbert damping for a higher magnetic field, $h = 5\mathcal{J}$. Under a strong magnetic field, the contribution of the perpendicular component of the Schwinger bosons almost vanishes, while that of the z' -component bosons becomes dominant. As a result, $\delta\alpha_G$ has only a single low-energy peak due to the flat part in the dispersion of the z' Schwinger bosons.

C. Clean interface under a finite magnetic field

Next, we show the result for the clean interface. In Fig. 5(a), we plot $\delta\alpha_G/\delta\alpha'_{G,0}$ as a function of the FMR frequency ω_0 , where $\delta\alpha'_{G,0} = 2\pi S_0 |\bar{T}|^2 / \mathcal{J}^2$. In contrast to the case of the dirty interface, the peak position depends on the magnetic field, reflecting the energy gap of the massive Schwinger boson, $\varepsilon_{\mathbf{k}z}$, at $\mathbf{k} = \mathbf{0}$. In Fig. 5(b), we present the increase of the Gilbert damping for $h = 3\mathcal{J}$ as a function of ω_0 and θ . In the case of

$\theta = \pi$, the Gilbert damping is not modulated, meaning $\delta\alpha_G = 0$. This is consistent with the fact that the coefficient becomes zero when $\theta = \pi$ and $\mathbf{k} = \mathbf{0}$ in Eq. (46). On the other hand, the peak becomes significant near $\theta = 0, 2\pi$.

V. SUMMARY

In this study, we examined spin pumping into a spin-nematic (SN) state in a junction system composed of a ferromagnetic insulator and a spin-nematic insulator. To clarify its qualitative features, we employed a spin-1 bilinear-biquadratic model to realize the spin-nematic phase and calculated the increase of the Gilbert damping using the mean-field theory based on the Schwinger boson formalism. We considered two types of interfaces—clean and dirty—using simple models with interfacial exchange coupling, both with and without momentum conservation. In the absence of a magnetic field, spin pumping is completely suppressed for a clean interface. However, for a dirty interface, the increase of the Gilbert damping exhibits a peak structure with a low-energy shoulder as a function of the FMR frequency, reflecting the energy dispersion of the two Schwinger bosons. The orientation angle of boson condensation also influences the increase of the Gilbert damping. In the presence of the magnetic field, the different angular dependence of the two kinds of bosons becomes more pronounced for a dirty interface, and the peak structure of the increase of Gilbert damping exhibits a complex dependence on the magnetic field orientation. For a clean interface, on the other hand,

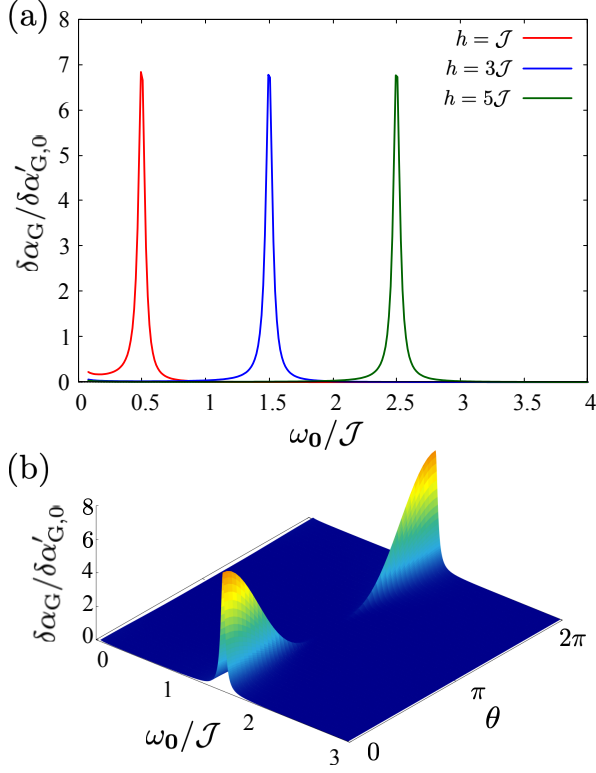


FIG. 5. The increase of the Gilbert damping for the clean interface as a function of the FMR frequency ω_0 for $J_1 = 0$, $J_2 = -\mathcal{J}$. (a) The magnetic-field dependence for $\theta = 0$. The three curves correspond to $h = \mathcal{J}$, $3\mathcal{J}$, and $5\mathcal{J}$, respectively. (b) The angle dependence for $h = 3\mathcal{J}$.

the increase of the Gilbert damping is governed by the energy gap of one of the two Schwinger boson modes at zero wavenumber and exhibits a single peak with strong dependence on the magnetic field orientation. Our results will be helpful in identifying the spin-nematic phase through spin pumping, a widely used technique in spintronics research.

ACKNOWLEDGEMENTS

The authors thank M. Matsuo for his helpful discussions. T. I. is supported by the International Graduate Program of Innovation for Intelligent World (IIW) of the University of Tokyo and the International Program of Institute for Solid State Physics, the University of Tokyo. T. K. acknowledges the support of the Japan Society for the Promotion of Science (JSPS KAKENHI Grant No. JP20K03831).

Appendix A: Detailed calculation of the spin-spin correlation function

In this appendix, we provide a detailed calculation of the spin-spin correlation functions. We first rewrite the spin operators in the (x', y', z') coordinate system using the Schwinger bosons, following Eqs. (6)-(8). We then apply the transformation given in Eq. (10) and the condensation condition for the parallel component boson, given in Eq. (11). As a result, the spin operators are calculated as

$$S_i^{+'} = i\sqrt{M} \left[\left(\cos \frac{\mu}{2} - \sin \frac{\mu}{2} \right) a_{z'}^\dagger(i) - \left(\cos \frac{\mu}{2} + \sin \frac{\mu}{2} \right) a_{z'}(i) \right], \quad (A1)$$

$$S_i^{z'} = M \sin \mu + i\sqrt{M} \cos \mu [a_{\perp}(i) - a_{\perp}^\dagger(i)], \quad (A2)$$

and $S_i^{-'} = (S_i^{+'})^\dagger$. Here, we have omitted higher-order terms with respect to $1/M$. By performing the Fourier transformation and the Bogoliubov transformation given in Eqs. (19) and (20), we obtain

$$S_{\mathbf{k}}^{+'} = i\sqrt{M} [(C_{\mu}^- c_{\mathbf{k}}^z - C_{\mu}^+ s_{\mathbf{k}}^z) \alpha_{\mathbf{k}z}^\dagger + (C_{\mu}^- s_{\mathbf{k}}^z - C_{\mu}^+ c_{\mathbf{k}}^z) \alpha_{-\mathbf{k}z}], \quad (A3)$$

$$S_{\mathbf{k}}^{z'} = M \sin \mu + i \cos \mu \sqrt{M} (c_{\mathbf{k}}^\perp - s_{\mathbf{k}}^\perp) [(\alpha_{-\mathbf{k}\perp} - \alpha_{\mathbf{k}\perp}^\dagger)], \quad (A4)$$

and $S_{\mathbf{k}}^{-'} = (S_{-\mathbf{k}}^{+'})^\dagger$, where $C_{\mu}^{\pm} = \cos(\mu/2) \pm \sin(\mu/2)$, $c_{\mathbf{k}}^\nu = \cosh \xi_{\mathbf{k}\nu}$, and $s_{\mathbf{k}}^\nu = \sinh \xi_{\mathbf{k}\nu}$. Using these operators, the spin-spin correlation functions are calculated as

$$\chi_{\mathbf{k}, -\mathbf{k}}^{+' -'}(\tau) = M [(C_{\mu}^- s_{\mathbf{k}}^z - C_{\mu}^+ c_{\mathbf{k}}^z)^2 G_{\mathbf{k}z}(\tau) + (C_{\mu}^- c_{\mathbf{k}}^z - C_{\mu}^+ s_{\mathbf{k}}^z)^2 G_{\mathbf{k}z}(-\tau)], \quad (A5)$$

$$\chi_{\mathbf{k}, -\mathbf{k}}^{-' +'}(\tau) = M [(C_{\mu}^- c_{\mathbf{k}}^z - C_{\mu}^+ s_{\mathbf{k}}^z)^2 G_{\mathbf{k}z}(\tau) + (C_{\mu}^- s_{\mathbf{k}}^z - C_{\mu}^+ c_{\mathbf{k}}^z)^2 G_{\mathbf{k}z}(-\tau)], \quad (A6)$$

$$\chi_{\mathbf{k}, -\mathbf{k}}^{+' +'}(\tau) = \chi_{\mathbf{k}, -\mathbf{k}}^{-' -'}(\tau) = -M [(C_{\mu}^- c_{\mathbf{k}}^z - C_{\mu}^+ s_{\mathbf{k}}^z)(C_{\mu}^- s_{\mathbf{k}}^z - C_{\mu}^+ c_{\mathbf{k}}^z)] [G_{\mathbf{k}z}(\tau) + G_{\mathbf{k}z}(-\tau)], \quad (A7)$$

$$\chi_{\mathbf{k}, -\mathbf{k}}^{z' z'}(\tau) = M \cos^2 \mu (c_{\mathbf{k}}^\perp - s_{\mathbf{k}}^\perp)^2 [G_{\mathbf{k}z}(\tau) + G_{\mathbf{k}z}(-\tau)], \quad (A8)$$

where $G_{\mathbf{k}\nu}(\tau)$ is a propagator of the Schwinger bosons defined by

$$G_{\mathbf{k}\nu}(\tau) = -\frac{1}{\hbar} \langle \alpha_{\mathbf{k}\nu}(\tau) \alpha_{\mathbf{k}\nu}^\dagger(0) \rangle. \quad (A9)$$

Using the diagonalized Hamiltonian, Eq. (22), this propagator is calculated as

$$G_{\mathbf{k}\nu}(i\omega_n) = \int_0^{\hbar\beta} d\tau e^{i\omega_n\tau} G_{\mathbf{k}\nu}(\tau) = \frac{1}{i\hbar\omega_n - \varepsilon_{\mathbf{k}\nu}}. \quad (\text{A10})$$

Combining these results with Eq. (33), it is straightforward to derive the final result for $\omega_0 > 0$, which is given in Eqs. (43)-(45).

[1] Y. Tserkovnyak, A. Brataas, and G. E. W. Bauer, Enhanced gilbert damping in thin ferromagnetic films, *Phys. Rev. Lett.* **88**, 117601 (2002).

[2] E. Šimánek and B. Heinrich, Gilbert damping in magnetic multilayers, *Phys. Rev. B* **67**, 144418 (2003).

[3] I. Žutić, J. Fabian, and S. Das Sarma, Spintronics: Fundamentals and applications, *Rev. Mod. Phys.* **76**, 323 (2004).

[4] Y. Tserkovnyak, A. Brataas, G. E. W. Bauer, and B. I. Halperin, Nonlocal magnetization dynamics in ferromagnetic heterostructures, *Rev. Mod. Phys.* **77**, 1375 (2005).

[5] F. Hellman, A. Hoffmann, Y. Tserkovnyak, G. S. D. Beach, E. E. Fullerton, C. Leighton, A. H. MacDonald, D. C. Ralph, D. A. Arena, H. A. Dürr, P. Fischer, J. Grollier, J. P. Heremans, T. Jungwirth, A. V. Kimel, B. Koopmans, I. N. Krivorotov, S. J. May, A. K. Petford-Long, J. M. Rondinelli, N. Samarth, I. K. Schuller, A. N. Slavin, M. D. Stiles, O. Tchernyshyov, A. Thiaville, and B. L. Zink, Interface-induced phenomena in magnetism, *Rev. Mod. Phys.* **89**, 025006 (2017).

[6] E. Y. Tsymbal and I. Žutić, eds., *Spintronics Handbook, Second Edition: Spin Transport and Magnetism* (CRC Press, 2019).

[7] W. Han, S. Maekawa, and X. Xie, Spin current as a probe of quantum materials, *Nat. Mater.* **19**, 139–152 (2020).

[8] F. Yang and P. C. Hammel, Fmr-driven spin pumping in y3fe5o12-based structures, *J. Phys. D Appl. Phys.* **51**, 253001 (2018).

[9] Z. Qiu, J. Li, D. Hou, E. Arenholz, A. T. N'Diaye, A. Tan, K.-i. Uchida, K. Sato, S. Okamoto, Y. Tserkovnyak, Z. Q. Qiu, and E. Saitoh, Spin-current probe for phase transition in an insulator, *Nat. Commun.* **7**, 1 (2016).

[10] T. Yamamoto, T. Kato, and M. Matsuo, Spin current at a magnetic junction as a probe of the Kondo state, *Phys. Rev. B* **104**, L121401 (2021).

[11] Y. Ominato and M. Matsuo, Quantum oscillations of gilbert damping in ferromagnetic/graphene bilayer systems, *J. Phys. Soc. Jpn.* **89**, 053704 (2020).

[12] Y. Ominato, J. Fujimoto, and M. Matsuo, Valley-dependent spin transport in monolayer transition-metal dichalcogenides, *Phys. Rev. Lett.* **124**, 166803 (2020).

[13] M. Yama, M. Tatsuno, T. Kato, and M. Matsuo, Spin pumping of two-dimensional electron gas with rashba and dresselhaus spin-orbit interactions, *Phys. Rev. B* **104**, 054410 (2021).

[14] M. Inoue, M. Ichioka, and H. Adachi, Spin pumping into superconductors: A new probe of spin dynamics in a superconducting thin film, *Phys. Rev. B* **96**, 024414 (2017).

[15] M. A. Silaev, Finite-frequency spin susceptibility and spin pumping in superconductors with spin-orbit relaxa-
tion, *Phys. Rev. B* **102**, 144521 (2020).

[16] M. A. Silaev, Large enhancement of spin pumping due to the surface bound states in normal metal–superconductor structures, *Phys. Rev. B* **102**, 180502(R) (2020).

[17] H. T. Simensen, L. G. Johnsen, J. Linder, and A. Brataas, Spin pumping between noncollinear ferromagnetic insulators through thin superconductors, *Phys. Rev. B* **103**, 024524 (2021).

[18] E. H. Fyhn and J. Linder, Spin pumping in superconductor-antiferromagnetic insulator bilayers, *Phys. Rev. B* **103**, 134508 (2021).

[19] Y. Ominato, A. Yamakage, T. Kato, and M. Matsuo, Ferromagnetic resonance modulation in *d*-wave superconductor/ferromagnetic insulator bilayer systems, *Phys. Rev. B* **105**, 205406 (2022).

[20] Y. Ominato, A. Yamakage, and M. Matsuo, Anisotropic superconducting spin transport at magnetic interfaces, *Phys. Rev. B* **106**, L161406 (2022).

[21] T. Funato, T. Kato, and M. Matsuo, Spin pumping into anisotropic dirac electrons, *Phys. Rev. B* **106**, 144418 (2022).

[22] C. Sun and J. Linder, Spin pumping from a ferromagnetic insulator to an unconventional superconductor with interfacial Andreev bound states, *Phys. Rev. B* **107**, 144504 (2023).

[23] H. Funaki, A. Yamakage, and M. Matsuo, Anisotropic spin-current spectroscopy of ferromagnetic superconducting gap symmetries, *Phys. Rev. B* **107**, 184437 (2023).

[24] C. Sun and J. Linder, Spin pumping from a ferromagnetic insulator into an altermagnet, *Phys. Rev. B* **108**, L140408 (2023).

[25] M. Yama, M. Matsuo, and T. Kato, Effect of vertex corrections on the enhancement of gilbert damping in spin pumping into a two-dimensional electron gas, *Phys. Rev. B* **107**, 174414 (2023).

[26] K. Fukuzawa, T. Kato, M. Matsuo, T. Jonckheere, J. Rech, and T. Martin, Spin pumping into carbon nanotubes, *Phys. Rev. B* **108**, 134429 (2023).

[27] S. Haddad, T. Kato, J. Zhu, and L. Mandhour, Twisted bilayer graphene reveals its flat bands under spin pumping, *Phys. Rev. B* **108**, L121101 (2023).

[28] B. M. and Y. Y. Hsieh, Biquadratic exchange and quadrupolar ordering, *Journal of Applied Physics* **40**, 1249 (1969).

[29] H. H. Chen and P. M. Levy, Quadrupole phase transitions in magnetic solids, *Phys. Rev. Lett.* **27**, 1383 (1971).

[30] A. Andreev and I. Grishchuk, Spin nematics, *Sov. Phys. JETP* **60** (1984).

[31] N. Papanicolaou, Unusual phases in quantum spin-1 sys-

tems, *Nuclear Physics B* **305**, 367 (1988).

[32] A. T. K. Tanaka and T. Idogaki, Long-range order in the ground state of the $s = 1$ isotropic bilinear-biquadratic exchange hamiltonian, *Journal of Physics A: Mathematical and General* **34**, 8767 (2001).

[33] S. Bhattacharjee, V. B. Shenoy, and T. Senthil, Possible ferro-spin nematic order in NiGa_2S_4 , *Phys. Rev. B* **74**, 092406 (2006).

[34] A. Läuchli, F. Mila, and K. Penc, Quadrupolar phases of the $s = 1$ bilinear-biquadratic heisenberg model on the triangular lattice, *Phys. Rev. Lett.* **97**, 087205 (2006).

[35] H. Tsunetsugu and M. Arikawa, Spin nematic phase in $s=1$ triangular antiferromagnets, *Journal of the Physical Society of Japan* **75**, 083701 (2006).

[36] P. Li, G.-M. Zhang, and S.-Q. Shen, $\text{Su}(3)$ bosons and the spin nematic state on the spin-1 bilinear-biquadratic triangular lattice, *Phys. Rev. B* **75**, 104420 (2007).

[37] H. Tsunetsugu and M. Arikawa, The spin nematic state in triangular antiferromagnets, *Journal of Physics: Condensed Matter* **19**, 145248 (2007).

[38] A. V. Chubukov, Chiral, nematic, and dimer states in quantum spin chains, *Phys. Rev. B* **44**, 4693 (1991).

[39] N. Shannon, T. Momoi, and P. Sindzingre, Nematic order in square lattice frustrated ferromagnets, *Phys. Rev. Lett.* **96**, 027213 (2006).

[40] H. T. Ueda and K. Totsuka, Ground-state phase diagram and magnetic properties of a tetramerized spin-1/2 J_1-J_2 model: Bec of bound magnons and absence of the transverse magnetization, *Phys. Rev. B* **76**, 214428 (2007).

[41] T. Vekua, A. Honecker, H.-J. Mikeska, and F. Heidrich-Meissner, Correlation functions and excitation spectrum of the frustrated ferromagnetic spin- $\frac{1}{2}$ chain in an external magnetic field, *Phys. Rev. B* **76**, 174420 (2007).

[42] T. Hikihara, L. Kecke, T. Momoi, and A. Furusaki, Vector chiral and multipolar orders in the spin- $\frac{1}{2}$ frustrated ferromagnetic chain in magnetic field, *Phys. Rev. B* **78**, 144404 (2008).

[43] M. Sato, T. Momoi, and A. Furusaki, Nmr relaxation rate and dynamical structure factors in nematic and multipolar liquids of frustrated spin chains under magnetic fields, *Phys. Rev. B* **79**, 060406 (2009).

[44] J. Sudan, A. Lüscher, and A. M. Läuchli, Emergent multipolar spin correlations in a fluctuating spiral: The frustrated ferromagnetic spin- $\frac{1}{2}$ heisenberg chain in a magnetic field, *Phys. Rev. B* **80**, 140402 (2009).

[45] M. E. Zhitomirsky and H. Tsunetsugu, Magnon pairing in quantum spin nematic, *Europhysics Letters* **92**, 37001 (2010).

[46] M. Sato, T. Hikihara, and T. Momoi, Field and temperature dependence of nmr relaxation rate in the magnetic quadrupolar liquid phase of spin- $\frac{1}{2}$ frustrated ferromagnetic chains, *Phys. Rev. B* **83**, 064405 (2011).

[47] R. Shindou, S. Yunoki, and T. Momoi, Projective studies of spin nematics in a quantum frustrated ferromagnet, *Phys. Rev. B* **84**, 134414 (2011).

[48] T. Momoi, P. Sindzingre, and K. Kubo, Spin nematic order in multiple-spin exchange models on the triangular lattice, *Phys. Rev. Lett.* **108**, 057206 (2012).

[49] M. Sato, T. Hikihara, and T. Momoi, Spin-nematic and spin-density-wave orders in spatially anisotropic frustrated magnets in a magnetic field, *Phys. Rev. Lett.* **110**, 077206 (2013).

[50] H. T. Ueda and T. Momoi, Nematic phase and phase separation near saturation field in frustrated ferromagnets, *Phys. Rev. B* **87**, 144417 (2013).

[51] S. Jiang, J. Romhányi, S. R. White, M. E. Zhitomirsky, and A. L. Chernyshev, Where is the quantum spin nematic?, *Phys. Rev. Lett.* **130**, 116701 (2023).

[52] T. Momoi and K. Totsuka, Magnetization plateaus of the shastry-sutherland model for $\text{SrCu}_2(\text{BO}_3)_2$: spin-density wave, supersolid, and bound states, *Phys. Rev. B* **62**, 15067 (2000).

[53] Z. Wang and C. D. Batista, Dynamics and instabilities of the shastry-sutherland model, *Phys. Rev. Lett.* **120**, 247201 (2018).

[54] Y. Yokoyama and C. Hotta, Spin nematics next to spin singlets, *Phys. Rev. B* **97**, 180404 (2018).

[55] T. Hikihara, T. Misawa, and T. Momoi, Spin nematics in frustrated spin-dimer systems with bilayer structure, *Phys. Rev. B* **100**, 214414 (2019).

[56] N. Büttgen, K. Nawa, T. Fujita, M. Hagiwara, P. Kuhns, A. Prokofiev, A. P. Reyes, L. E. Svistov, K. Yoshimura, and M. Takigawa, Search for a spin-nematic phase in the quasi-one-dimensional frustrated magnet licuvo_4 , *Phys. Rev. B* **90**, 134401 (2014).

[57] A. Orlova, E. L. Green, J. M. Law, D. I. Gorbunov, G. Chanda, S. Krämer, M. Horvatić, R. K. Kremer, J. Wosnitza, and G. L. J. A. Rikken, Nuclear magnetic resonance signature of the spin-nematic phase in licuvo_4 at high magnetic fields, *Phys. Rev. Lett.* **118**, 247201 (2017).

[58] M. Yoshida, K. Nawa, H. Ishikawa, M. Takigawa, M. Jeong, S. Krämer, M. Horvatić, C. Berthier, K. Matsui, T. Goto, S. Kimura, T. Sasaki, J. Yamaura, H. Yoshida, Y. Okamoto, and Z. Hiroi, Spin dynamics in the high-field phases of volborthite, *Phys. Rev. B* **96**, 180413 (2017).

[59] R. Nath, A. A. Tsirlin, H. Rosner, and C. Geibel, Magnetic properties of $\text{BaCdVO}(\text{PO}_4)_2$: A strongly frustrated spin- $\frac{1}{2}$ square lattice close to the quantum critical regime, *Phys. Rev. B* **78**, 064422 (2008).

[60] M. Skoulatos, F. Rucker, G. J. Nilsen, A. Bertin, E. Pomjakushina, J. Ollivier, A. Schneidewind, R. Georgii, O. Zaharko, L. Keller, C. Rüegg, C. Pfleiderer, B. Schmidt, N. Shannon, A. Kriele, A. Senyshyn, and A. Smerald, Putative spin-nematic phase in $\text{BaCdVO}(\text{PO}_4)_2$, *Phys. Rev. B* **100**, 014405 (2019).

[61] K. Y. Povarov, V. K. Bhartiya, Z. Yan, and A. Zheludev, Thermodynamics of a frustrated quantum magnet on a square lattice, *Phys. Rev. B* **99**, 024413 (2019).

[62] D. Hirobe, M. Sato, M. Hagiwara, Y. Shiomi, T. Masuda, and E. Saitoh, Magnon pairs and spin-nematic correlation in the spin seebeck effect, *Phys. Rev. Lett.* **123**, 117202 (2019).

[63] C. Lacroix, P. Mendels, and F. Mila, *Introduction to Frustrated Magnetism: Materials, Experiments, Theory*, Springer Series in Solid-State Sciences (Springer Berlin Heidelberg, 2011).